Vibrational Energy Flow in Carbon Composite Structures

Mariam JABER[1]; Helmut SCHNEEWEISS[1]; Joachim BÖS[2]; Tobias MELZ[2]

[1] BMW Group, Germany

[2] Technische Universität Darmstadt, Germany

ABSTRACT

Structures made from carbon composite materials are rapidly replacing metallic ones in the automotive industry because of their high strength-to-mass ratio. The goal of this study is to enhance acoustic comfort of cars made from carbon composites by comparing various carbon composites in order to find the most suitable composite in terms of mechanical and dynamic properties. To achieve this goal, the structural intensity method is implemented. This method can give information concerning the paths of energy propagated through structures and the localization of vibration sources and sinks. The significance of the present research is that it takes into account the effect of the material damping on the dissipation of the energy in a structure. The damping of the composite is presented as a function of its macro mechanical properties, frequency, geometry, and boundary conditions. The damping values are calculated from a 2D analytical model based on the laminate theory and the modal strain energy method. The benefit of this research for acoustics is that it demonstrates the effect of material properties on the passive control of vibrations in a structure. Consequently, vibrational energy propagated in carbon composite structures is reduced, and less noise is radiated.

Keywords: NVH, composite structures   I-INCE Classification of Subjects Number(s): 13.2.1

1. INTRODUCTION

In order to improve the NVH (noise, vibrations, and harshness) performance of future vehicles without increasing production cost or weight, the effect of material properties on passive control of vibrations in CFRP (carbon fiber reinforced plastic) structures is investigated. In order to find suitable composite lay-ups in terms of NVH performance, the damping of various carbon composite laminas is simulated numerically. The paths of energy propagated through carbon composite structures and the location of vibration sources and sinks are determined. The effect of material damping on the dissipation of vibrational energy is taken into account. The dependence of damping on frequency and material orientation is studied and, thus, the NVH performance of carbon composites can be improved. In this paper, firstly the structural intensity method of carbon composite laminas is implemented, then a study of the effect of the modal damping on the vibrational energy flow is performed. Finally, the modal strain energy method is implemented to determine the accurate values of modal damping of a vibrating structure.

2. CALCULATION OF STRUCTURAL INTENSITY OF LAMINATED PLATES

The structural intensity represents the vibrational power flow per unit cross-sectional area of a dynamically loaded structure. Since Noiseux (1) introduced the measurement method of power flow in beams and plates using measured accelerations and the wave equation, many studies have been carried out over the years to understand power flow phenomena in structures. For instance, Pavic (2), Fahy and Pierri (3), and Verheij (4) presented the measurement methods of vibration power flow using the measured amplitudes in frequency and or time domain, and they estimated the internal forces numerically by the finite difference method. Structural intensity analysis using the finite element method (FEM) was also formulated by Gavric, and Pavic (5) and by Hambric (6). Using FEM simulations, Rajmani et al. (7) studied the dynamic response of composite laminas with cutouts for simply supported and clamped boundary conditions. Lee et al. (8) studied the free vibration of composite laminas with rectangular cutouts. Liu (9) studied the structural intensity characteristics of isotropic plates under low-velocity impact. Wang et al. (10) studied the structural intensity characteristics

---

[1] mariam.jaber@bmw.de

[2] boes@szm.tu-darmstadt.de

of composite laminas subjected to a dynamic concentrated force. Wang et al. (11) discussed the structural intensity characteristics of composite laminas subjected to impact load.

The instantaneous structural intensity component in the time domain is defined as follows

$$i_k(t) = -\sigma_{kl}(t)v_l(t) \tag{1}$$

where $\sigma_{kl}(t)$ and $v_l(t)$ are the stress and velocity, respectively, in the l-direction at time t. The temporal mean of the kth instantaneous intensity component $I_k = <i_k(t)>$ represents the net energy flow through the structure. For steady-state vibrations the complex structural intensity can be defined as (13)

$$\prod_k(\omega) = \frac{1}{2}\widetilde{\sigma}_{kl}(\omega)\widetilde{v}_l^*(\omega) = I_k(\omega) + jJ_k(\omega), \; k,l = 1,2,3, \tag{2}$$

where ω is the $frequency, \widetilde{v}_l^*(\omega)$ is the complex conjugate of velocity and $\widetilde{\sigma}_{kl}(\omega)$ is the complex stress. The real part of the quantity $I_k(\omega)$ is called active intensity and indicates the net energy flow in the structure. The imaginary part $J_k(\omega)$ is called reactive intensity and does not contribute to the net energy flow in a structure. The active intensity is associated with propagative vibration fields. For composite laminated plate elements, since stresses and displacements are usually determined as stress results and movements for each layer, the integration is carried out over the whole thickness. The structural intensity in the laminated plates can be expressed in the form of power flow per unit width. Both flexural deformations and membrane effect are considered in the formulation of the reactive structural intensity of the plate. The two-dimensional components of the active and reactive structural intensity in the local x and y directions for a vibrating flat plate can be expressed as (5)

$$I_{reactive\,x} = -\frac{\omega}{2}Imag[\widetilde{N}_x\widetilde{u}^* + \widetilde{N}_{xy}\widetilde{v}^* + \widetilde{Q}_x\widetilde{W}^* + \widetilde{M}_x\widetilde{\theta}_y^* - \widetilde{M}_{xy}\widetilde{\theta}_x^*], \tag{3}$$

$$I_{reactive\,y} = -\frac{\omega}{2}Imag[\widetilde{N}_y\widetilde{v}^* + \widetilde{N}_{yx}\widetilde{u}^* + \widetilde{Q}_y\widetilde{W}^* - \widetilde{M}_y\widetilde{\theta}_x^* + \widetilde{M}_{yx}\widetilde{\theta}_y^*], \tag{4}$$

$$I_{active\,x} = -\frac{\omega}{2}Real[\widetilde{N}_x\widetilde{u}^* + \widetilde{N}_{xy}\widetilde{v}^* + \widetilde{Q}_x\widetilde{W}^* + \widetilde{M}_x\widetilde{\theta}_y^* - \widetilde{M}_{xy}\widetilde{\theta}_x^*], \tag{5}$$

$$I_{active\,y} = -\frac{\omega}{2}Real[\widetilde{N}_y\widetilde{v}^* + \widetilde{N}_{yx}\widetilde{u}^* + \widetilde{Q}_y\widetilde{W}^* - \widetilde{M}_y\widetilde{\theta}_x^* + \widetilde{M}_{yx}\widetilde{\theta}_y^*], \tag{6}$$

where $\widetilde{N}_x$, $\widetilde{N}_y$, and $\widetilde{N}_{xy} = \widetilde{N}_{yx}$ are complex membrane forces per unit width of plate, $\widetilde{M}_x$, $\widetilde{M}_y$, and $\widetilde{M}_{xy} = \widetilde{M}_{yx}$ are complex bending and twisting moments per unit width of plate, $\widetilde{Q}_x$ and $\widetilde{Q}_y$ are complex transverse shear forces per unit width of plate, $\widetilde{u}^*$, $\widetilde{v}^*$, and $\widetilde{W}^*$ are complex conjugates of translational displacements in x, y, and z directions, $\widetilde{\theta}_x^*$, and $\widetilde{\theta}_x^*$ are complex conjugates of rotational displacements about x and y directions. For the composite laminas, the stress-strain relation for an orthotropic layer in any orientation angle in the plane of the layer k is given as

$$\begin{Bmatrix} \sigma_x^k \\ \sigma_y^k \\ \tau_{xy}^k \end{Bmatrix} = \begin{bmatrix} C_{11}^k & C_{21}^k & C_{61}^k \\ C_{12}^k & C_{22}^k & C_{62}^k \\ C_{16}^k & C_{26}^k & C_{66}^k \end{bmatrix} \cdot \begin{Bmatrix} \varepsilon_x^k \\ \varepsilon_y^k \\ \gamma_{xy}^k \end{Bmatrix}, \tag{7}$$

where the transformed stiffness $C_{ij} = C_{ji}$ is given in terms of the orientation angle and the engineering constants of the material. For small deformations the displacement components of a point are

$$u = u_0 - z\omega_{,x}, \tag{8}$$

$$v = v_0 - z\omega_{,y}. \tag{9}$$

The strain-displacement relations are

$$\varepsilon_x = u_{0,x} - zW_{,xx},$$
$$\varepsilon_y = v_{0,y} - zW_{,yy}, \tag{10}$$
$$\gamma_{xy} = u_{0,y} + v_{0,x} - 2z\omega_{,yy}.$$

For a typical lamina k, the contribution of this lamina to the stress-resultants and stress couples of the plate is given by

$$\left. \begin{cases} N_x = \int_{h_{k-1}}^{h_k} \sigma_x \mathrm{d}z \\[2mm] N_y = \int_{h_{k-1}}^{h_k} \sigma_y \mathrm{d}z \\[2mm] N_{xy} = \int_{h_{k-1}}^{h_k} \tau_{xy} \mathrm{d}z \\[2mm] M_x = \int_{h_{k-1}}^{h_k} \sigma_x z \mathrm{d}z \\[2mm] M_y = \int_{h_{k-1}}^{h_k} \sigma_y z \mathrm{d}z \\[2mm] M_{xy} = \int_{h_{k-1}}^{h_k} \tau_{xy} z \mathrm{d}z \end{cases} \right\} . \tag{11}$$

Thus, if there are n laminas in the plate, the stress resultants and stress couples are obtained by simply summing Eq. (11) over the n laminas, substituting Eqs. (10) and (7) in Eq. (11), and performing this summation results in

$$\begin{Bmatrix} N_x \\ N_y \\ N_{xy} \end{Bmatrix} = \begin{bmatrix} A11^k & A_{21}^k & A_{61}^k \\ A_{12}^k & A_{22}^k & A_{62}^k \\ A_{16}^k & A_{26}^k & A_{66}^k \end{bmatrix} \cdot \begin{Bmatrix} u_{0,x} \\ v_{0,y} \\ u_{0,y} + v_{0,x} \end{Bmatrix} - \begin{bmatrix} B11^k & B_{21}^k & B_{61}^k \\ B_{12}^k & B_{22}^k & B_{62}^k \\ B_{16}^k & B_{26}^k & B_{66}^k \end{bmatrix} \cdot \begin{Bmatrix} w_{,xx} \\ w_{,yy} \\ 2w_{,xy} \end{Bmatrix}$$

for the stress resultants and in

$$\begin{Bmatrix} M_x \\ M_y \\ M_{xy} \end{Bmatrix} = \begin{bmatrix} B11 & B_{21} & B_{61} \\ B_{12} & B_{22} & B_{62} \\ B_{16} & B_{26} & B_{66} \end{bmatrix} \cdot \begin{Bmatrix} u_{0,x} \\ v_{0,y} \\ u_{0,y} + v_{0,x} \end{Bmatrix} - \begin{bmatrix} D_{11} & D_{21} & D_{61} \\ D_{12} & D_{22} & D_{62} \\ D_{16} & D_{26} & D_{66} \end{bmatrix} \cdot \begin{Bmatrix} w_{,xx} \\ w_{,yy} \\ 2w_{,xy} \end{Bmatrix}$$

for the stress couples, where the A_{ij}, B_{ij} and D_{ij} are defined by

$$\begin{aligned} A_{ij} &= \sum_{k=1}^{n} C_{ij}^k (h_k - h_{k-1}), \\ B_{ij} &= \frac{1}{2} \sum_{k=1}^{n} C_{ij}^k (h_k^2 - h_{k-1}^2), \\ D_{ij} &= \frac{1}{3} \sum_{k=1}^{n} C_{ij}^k (h_k^3 - h_{k-1}^3). \end{aligned} \tag{12}$$

3. DAMPING ANALYSIS OF COMPOSITE STRUCTURES

Generally, vehicles are subjected to dynamic loadings, and if they are not properly designed they may fail due to instability or fatigue. Therefore, the area of dynamic behavior of fiber reinforced composite structures has attracted close attention in the recent years. In particular, since damping has the beneficial effect of absorbing noise and vibrations of the system, the studies of damping capacities of laminated structures have been carried out by many investigators. The damping in a structure helps to reduce the amplitudes of the vibrations of the structure, and, consequently, it is considered a very important feature in mechanical design.

In general, the damping in metal structures is low, which results in high amplitudes of the vibrations. For carbon composite materials, damping is higher, and it depends on the constitution of the materials. From micro mechanical point of view, the energy dissipation in carbon fiber reinforced composites is induced by various processes such as the viscoelastic behavior of the matrix and the damping of the fiber-matrix interface. From a macro mechanical point of view, the damping depends on the constituent layer properties, layer orientations, inter-laminar effects, and stacking sequence. Moreover, the damping in composites involves a variety of energy dissipation mechanisms that depend on vibrational parameters such as frequency, amplitude, and environmental conditions such as temperature and moisture. Vance et al. (14) reviewed in detail the initial works on the damping analysis of fiber composite materials. Adams and Bacon (15) did a damping analysis of composite materials in which the energy dissipation can be described as separable energy dissipations associated with the individual stress components. Afterwards, this analysis was refined by Ni and Adams (16). The damping of orthotropic beams is presented as a function of material orientation. Moreover, the damping of cross-ply laminas, angle-ply laminas, as well as more general types of symmetric laminates were studied. Adams and Maheri (17) applied the damping concept of Adams and Bacon to the investigation of angle-ply laminas made of unidirectional glass fiber or carbon layers. Lin et al. (18) and Maheri and Adams (19) used the finite element analysis to evaluate the damping properties of free-free fiber reinforced plates. The two transverse shear damping parameters were included in these analyses. Then, the established damping model of FRP composites by Adams and Maheri (17) named modal strain energy approach was adopted by the following authors in order to develop the damping analysis of various composites (20, 21, 22). Maheri et al. (23) also demonstrated that the modal strain energy method was effective for analyzing the vibration damping of honeycomb structure panels with carbon fiber composite sheets. Berthelot (24) studied extensively the damping of carbon composite laminas with viscoelastic layers and sandwich materials. Yang et al. (25) used the modal strain energy method to study the vibration and damping characteristics of hybrid carbon fiber composte pyramidal truss sandwich panels with viscoelastic layers. The various definitions of damping are related as follows (26)

$$\eta = \frac{\Psi}{2\pi} = 2\xi = \frac{1}{Q} = \frac{\delta}{\pi} = \frac{E_2}{E_1} = \tan\Phi \tag{13}$$

where η is the loss factor, ψ is the specific damping capacity, ξ is the damping ratio, Q is the quality factor, δ is the logarithmic decrement, E_1 is the storage modulus, E_2 is the loss modulus and Φ is the loss angle.

4.   MODAL STRAIN ENERGY APPROACH

In this paper, the modal strain energy approach was applied in a finite element formulation to calculate the damping properties of carbon composite laminas. The principle of this method is that the damping properties of a structure can be defined by the ratio of the energy dissipated to the energy stored during a stress cycle. For all CFRP laminas, the damping characteristics are obviously anisotropic. Hence, the total structural damping loss factor can be expressed as

$$\eta = \frac{\sum_{k=1}^{n} \eta_{ij} U_{ij}^k}{\sum_{k=1}^{n} U_{ij}^k} \ (i, j = 1, 2, 3), \tag{14}$$

where η_{ij} and U_{ij}^k are the damping loss factors of the composite parent material and the strain energy components of the element k respectively. The number 1 is the fiber direction. 2 is transverse to this direction, and 3 is through thickness direction. The strain energy U_{ij}^k is related to the stress component σ_{ij} and the strain component ε_{ij} as follows

$$U_{ij}^k = \frac{1}{2} \int \sigma_{ij}^k \varepsilon_{ij}^k dV^k. \tag{15}$$

4.0.1 In-Plane Strain Energy

All the layers of the composite materials considered in this study are constituted of orthotropic materials. In each layer, the stresses σ_1, σ_2, and σ_{12}, related to the material directions, can be expressed as functions of the in-plane stresses σ_{xx}, σ_{yy}, and σ_{xy}, related to the finite element directions (x, y, z), according to

$$\begin{bmatrix} \sigma_1 \\ \sigma_2 \\ \sigma_{12} \end{bmatrix} = \begin{bmatrix} \cos^2(\theta) & \sin^2(\theta) & 2\sin(\theta)\cos(\theta) \\ \sin^2(\theta) & \cos^2(\theta) & -2\sin(\theta)\cos(\theta) \\ -\sin(\theta)\cos(\theta) & \sin(\theta)\cos(\theta) & \cos^2(\theta) - \sin^2(\theta) \end{bmatrix} \begin{bmatrix} \sigma_{xx} \\ \sigma_{yy} \\ \sigma_{xy} \end{bmatrix}, \tag{16}$$

where θ is the orientation of material in layer. In a similar way, the strains ε_1, ε_2, and ε_{12}, related to the material directions, can be expressed as functions of the in-plane stresses ε_{xx}, ε_{yy}, and ε_{xy}, in the finite element directions (x, y, z), according to the stress transformation relation

$$
\begin{bmatrix} \varepsilon_1 \\ \varepsilon_2 \\ \varepsilon_{12} \end{bmatrix} = \begin{bmatrix} \cos^2(\theta) & \sin^2(\theta) & 2\sin(\theta)\cos(\theta) \\ \sin^2(\theta) & \cos^2(\theta) & -2\sin(\theta)\cos(\theta) \\ -\sin(\theta)\cos(\theta) & \sin(\theta)\cos(\theta) & \cos^2(\theta) - \sin^2(\theta) \end{bmatrix} \begin{bmatrix} \varepsilon_{xx} \\ \varepsilon_{yy} \\ \varepsilon_{xy} \end{bmatrix}. \tag{17}
$$

The total in-plane energy U_d^e stored in a given finite element e can be expressed as a function of the in-plane strain energies related to the material directions as

$$
U_d^e = U_{11}^e + U_{22}^e + U_{12}^e, \tag{18}
$$

with

$$
\begin{aligned}
U_{11}^e &= \frac{1}{2} \int \int \int \sigma_1^e \varepsilon_1^e \, dxdydz, \\
U_{22}^e &= \frac{1}{2} \int \int \int \sigma_2^e \varepsilon_2^e \, dxdydz, \\
U_{12}^e &= \frac{1}{2} \int \int \int \sigma_{12}^e \varepsilon_{12}^e \, dxdydz.
\end{aligned} \tag{19}
$$

The in-plane strain energies stored in the finite element e can be expressed as

$$
\begin{aligned}
U_{11}^e &= \sum_{k=1}^n U_{11k}^e, \\
U_{12}^e &= \sum_{k=1}^n U_{12k}^e, \\
U_{22}^e &= \sum_{k=1}^n U_{22k}^e.
\end{aligned} \tag{20}
$$

where U_{ijk}^e (ij=11,22,12) are the in-plane strain energies stored in the layer k of the element e, and n is the total number of layers in the laminate. Next, the total in-plane strain energies stored in the finite element assemblage are obtained by summation on the elements as

$$
\begin{aligned}
U_{11} &= \sum_{\text{elements}} U_{11}^e, \\
U_{12} &= \sum_{\text{elements}} U_{12}^e, \\
U_{22} &= \sum_{\text{elements}} U_{22}^e.
\end{aligned} \tag{21}
$$

Transverse Shear Strain Energy

The transverse shear strain energy for a given element e can be expressed in the material directions as

$$
U_s^e = U_{13}^e + U_{23}^e, \tag{22}
$$

with

$$
\begin{aligned}
U_{13}^e &= \frac{1}{2} \int \int \int \sigma_{13}^e \varepsilon_{13}^e \, dxdydz, \\
U_{23}^e &= \frac{1}{2} \int \int \int \sigma_{23}^e \varepsilon_{23}^e \, dxdydz,
\end{aligned} \tag{23}
$$

where the integration is extended over the volume of the finite element e. σ_{23} and ε_{23} are, respectively, the transverse shear stress and the strain in plane (2,3) of material in layer k. σ_{13} and ε_{13} are, respectively, the

transverse shear stress and the strain in the plane (1,3). In each layer k, the stresses σ_{13}, σ_{23} and the strains ε_{13}, ε_{23}, related to material directions of the layer, can be expressed, respectively, as a function of the transverse shear stresses σ_{yz}, σ_{yz} and a function of the transverse shear strains ε_{yz}, ε_{yz}, as

$$\begin{bmatrix} \sigma_{13} \\ \sigma_{23} \end{bmatrix} = \begin{bmatrix} \cos(\theta) & -\sin(\theta) \\ \sin(\theta) & \cos(\theta) \end{bmatrix} \begin{bmatrix} \sigma_{xz} \\ \sigma_{yz} \end{bmatrix}, \tag{24}$$

$$\begin{bmatrix} \varepsilon_{13} \\ \varepsilon_{23} \end{bmatrix} = \begin{bmatrix} \cos(\theta) & -\sin(\theta) \\ \sin(\theta) & \cos(\theta) \end{bmatrix} \begin{bmatrix} \varepsilon_{xz} \\ \varepsilon_{yz} \end{bmatrix}. \tag{25}$$

The transverse shear energies can be expressed as

$$U_{13}^e = \sum_{k=1}^n U_{13k}^e, $$
$$U_{23}^e = \sum_{k=1}^n U_{23k}^e, \tag{26}$$

where U_{ijk}^e (ij= 13, 23) are the transverse shear energies stored in the layer k of the element e. Next, the total transverse shear strain energies stored in the finite element assemblage are obtained by summation on the elements as

$$U_{13} = \sum_{\text{elements}} U_{13}^e, $$
$$U_{23} = \sum_{\text{elements}} U_{23}^e. \tag{27}$$

The total strain energy stored in the laminated structure is given by

$$U_{total} = U_{11} + U_{22} + U_{12} + U_{13} + U_{23}, \tag{28}$$

where the in-plane strain energies U_{11}, U_{22}, and U_{12} are expressed by Eq. (21), and the transverse shear strain energies U_{13}, and U_{23} are expressed by Eq. (27). U_{11}, U_{22} are the contributions of tension-compression deformation in the 1 and 2 direction of the fiber reinforced structures, respectively. U_{12}, U_{13} and U_{23} are the contributions of shear deformations in the planes (1,2), (1,3) and (2,3), respectively. Then, the energy dissipated by damping in the layer k of the element e is derived from the strain energy stored in the layer by introducing the specific damping coefficients ψ_{pqk}^e of each layer ψ_{pqk}^e as

$$\Delta U_k^e = \psi_{11k}^e U_{11k}^e + \psi_{12k}^e U_{12k}^e + \psi_{22k}^e U_{22k}^e + \psi_{13}^e U_{13}^e + \psi_{23}^e U_{23}^e. \tag{29}$$

These coefficients are related to the material directions (1,2,3) of the layer, ψ_{11k}^e and ψ_{22k}^e are the damping coefficients in traction-compression in the 1 direction and 2 direction of the layer, respectively, ψ_{12k}^e is the in-plane shear coefficient, ψ_{13k}^e and ψ_{23k}^e are the transverse shear damping coefficients in planes (2, 3) and (1,3), respectively. The damping energy dissipated in the element e is next obtained by summation on the layers of element e as

$$\Delta U^e = \sum_{k=1}^n \Delta U_k^e. \tag{30}$$

And the total energy ΔU dissipated in the finite element assemblage is then obtained by summation on the elements

$$\Delta U = \sum_{\text{elements}} \Delta U^e. \tag{31}$$

Finally, the total damping of the finite element assemblage is characterized by the damping coefficient ψ of the assemblage derived from the relation

$$\psi = \frac{\Delta U}{U_{total}}. \tag{32}$$

4.1 Procedure for Evaluating the Damping of Composite Structure

The procedure for evaluating the damping of carbon composite structure was performed by implementing a postprocessing tool for models simulated using two commercial finite element software packages, namely, Abaqus and Nastran. This procedure is based on the previous formulation, and it is valid for any structure in which the damping characteristics are different according to the layers and to the elements of the assemblage. Figure 1 shows the solution procedure of the damping loss factor of the model. The finite element analysis is used first to calculate the frequency response function of the vibrating structure. The natural frequencies and the corresponding mode shapes are obtained. For each frequency, the total number of layers is extracted. Then the thickness of each layer is extracted. Then for every element in each layer, the area and the components of stresses σ_{ij}^k and strains ε_{ij}^k are extracted in order to calculate and cumulate the various strain energies of the whole model. Then, the specific damping capacities of each layer are used to calculate the dissipated energy components. Finally, the damping of the whole carbon composite structure is calculated according to Eq. (32).

5.   MODEL VERIFICATION

In order to validate the implementation of this model, a test case is made and compared for the case of glass fibre composites. The specific damping capacities and the material properties of the single layers are taken from Adams and Maheri (17). A cantilever beam in a clamping block is excited at a point near the clamping block. The test is performed for glass fiber/epoxy laminas, E_{11}= 41.5 GPa, E_{22}= 10.9 GPa, G_{12}= 4.91 GPa, μ_{12}= 0.32, η_{11}=1.61 %, η_{22} = 6.7 %, and η_{12}=7.3 %. The frequency has been fixed at 50 Hz in order to test the effect of the fiber orientation on the loss factor. The beam is composed of 8 unidirectional layers of thickness 2 mm. The width-to-length ratio of the beam used is 1:17. The loss factor was tested for various fiber orientations between 0 and 90 degrees. The results were compared to the results of Adams and Maheri (17). A good agreement was found. The maximum of difference was found at 45 degrees, because in this 2D model the effect of the inter-laminar interface on the damping is not taken accurately. Figure 2 shows the results of this test. The model was also verified with a square plate of material-III given in (27). A square plate was tested in simply supported boundary conditions with the same dimensions given in (27). A good agreement was found in the variation of the specific damping capacity of a single layer with fiber orientation.

6.   RESULTS AND DISCUSSION

The dynamic mechanical behavior of a vibrating structure is governed by the material properties and by its geometrical dimensions. The material's elastic modulus measures its capacity to store mechanical strain energy, while its damping measures its capacity to dissipate energy. For instance, metallic materials are generally stiff and have a high elastic modulus. These materials can generate high mechanical strain energy, but they are poor in dissipating the energy because of low damping. Polymeric materials are viscoelastic, i.e., they have both viscous and elastic properties. A polymer component can absorb significant energy and can dissipate the energy. In order to study the effect of the damping on the structural intensity for a single natural frequency, several tests were performed for various geometries, frequencies, and boundary conditions. The material used in this section is HMS carbon epoxy (DX 210) (16). The results show that the influence of the damping is only quantitative, i.e. the directions of the vectors stayed the same and only their absolute values are affected. However, for the averaged structural intensity, the damping effect becomes also qualitative. The roof is tested in simply supported boundary conditions, firstly with a constant damping over the frequency domain [0 Hz – 600 Hz], and secondly with a variable damping depending on the frequency. The structural intensity is averaged over all natural frequencies present in this domain. The results show that in the case of averaged structural intensity, the variable damping can change also qualitatively the vibrational energy flow. Figure 3 shows the structural intensity distribution in the two cases. In order to study the effect of the boundary conditions on the damping the damping of a carbon composite square plate with the lay-up [45,–45,45,–45] was calculated in simply supported and clamped boundary conditions. Figure 4 shows the additionl damping added to the structure from the friction at the boundary conditions. The boundary conditions affected the amount of the energy absorbed in the different directions of the composites. For instance, for the third mode shape present at 351 Hz in clamped BC and for the fourth mode shape present at 388 Hz in simply supported BC. The distribution of the strain energy in the different directions of the composite is illustrated in Fig. 5 with $_{ij}$ is the strain energy stored in the direction (i,j). So two parameters play crucial role in the total damping of composite structure. The first one is the amount of energy stored in each direction in each layer, which can vary with the boundary conditions, fiber orientation, and the lay-up of the whole composite. The second one is the specific damping capacity of the single layer, which can be affected by the type of fibers used and the fiber volume fraction. Moreover, a study of the vibrational energy flow is done for a car's roof in free, simply supported, and ball-joint boundary conditions. In free boundary conditions the energy flow is more concentrated at the

boundaries. For simply supported and ball-joint boundary conditions, the energy flow has many virtual sinks that can dissipate the vibrational energy. This difference in the directions of the vibrational energy flow is the consequence of the different mode shapes coming from various boundary conditions. Figure 6 shows the variation of the vibrational energy flow with the boundary conditions. In order to study the effect of the layer orientation, the damping of four composite laminas is studied in the frequency domain [0 Hz–600 Hz]. Table 1 shows the various composite lay-ups and the engineering constants of each composite. The roof of the car is simulated for the four composites in simply supported boundary conditions. The mass of the roof is 6.69 kg and the thickness is 3 mm. Figure 7 shows the specific damping capacity curves calculated at the natural frequencies of each composite. By keeping the same mass and the same thickness of the roof, the using the

Table 1 – composite roofs properties

Composite	Lay-up	E_1 (GPa)	E_2 (GPa)	v_{12}	G_{12} (GPa)	mass (kg)	thickness (mm)
A	$[0,0,0]_2$	172	7.2	0.29	3.76	6.69	3
B	$[45,-45,45]_2$	13.9	13.9	0.84	43.910	6.69	3
C	$[0,30,60]_2$	85.778	37.23	0.52	23.835	6.69	3
D	$[0,15,30,45.60,75]$	74.854	50.181	0.39	23.835	6.69	3

same layers from the same material, and changing only the orientations of these layers, the dynamic properties of the composite change greatly. The engineering constants vary largely from composite to other and, the amount of energy stored in each direction varies, and, consequently, the loss factor of the whole composite structure vary from composite to other. The averaged vibrational flow is studied for the composites A, B, C, D mentioned in Table 1. The average is calculated over all the natural frequencies present in the frequency domain [0 Hz-600 Hz]. The same test is performed for a steel roof. Table 2 shows the properties of the roof made from steel. The structural intensity of the various composites and steel roofs is illustrated in Figure 8.

Table 2 – steel roof properties

material	E_1 (GPa)	v_{12}	mass (kg)	thickness (mm)
steel	210	0.29	7.43	0.7

The vibrational energy flow varies largely from composite to other. In this study, the elastic modulus of the carbon composite roofs is smaller than that of steel roof. Ultimately, the energy in the composite laminas flows easier than in the steel. From these results it can be seen that it is easy to change the number and the positions of virtual sources and sinks of the carbon composite roofs. In addition, as it is shown in Table 1, the distribution of the elastic modulus of the composite laminas is also influenced by the stacking sequence of the composite laminas. Consequently, the stacking sequence of the composite laminas affects the number of virtual sources and sinks of the energy flow.

7.   CONCLUSIONS

Damping in fiber reinforced composite materials is highly tailorable with respect to constituent properties such as ply orientation angles. Thus the properly designed structure can provide significant damping and may further improve the dynamic performance. The vibrational energy flow can be significantly reduced and the paths of the energy flow become smoother. The number of virtual sources and sinks can be largely affected. As the increased damping results in a decrease of stiffness, and strength, therefore any selection of material properties must be based on trade off between damping, stiffness and strength. The modal strain energy method is very effective to calculate the structural damping based on information on the parent material. The industrial application of this work will be to apply this method on the carbon composites used in the BMW group. An accurate measurement of the parent material damping allows to get an ideas about thousands of possible combinations in various boundary conditions. The calculated values of damping can be used then in the numerical simulations in order to get more accurate idea about the dynamic behavior of vibrating composite structures.

ACKNOWLEDGMENTS

REFERENCES

1. Noiseux D. Measurement of power flow in uniform beams and plates. The Journal of the Acoustical Society of America. 1970;47(1B):238–247.

2. Pavić G. Measurement of structure borne wave intensity, Part I: Formulation of the methods. Journal of Sound and Vibration. 1976;49(2):221–230.

3. Fahy F, Pierri R. Application of cross-spectral density to a measurement of vibration power flow between connected plates. The Journal of the Acoustical Society of America. 1977;62(5):1297–1298.

4. Verheij J. Cross spectral density methods for measuring structure borne power flow on beams and pipes. Journal of Sound and Vibration. 1980;70(1):133–138.

5. Gavrić L, Pavić G. A finite element method for computation of structural intensity by the normal mode approach. Journal of Sound and Vibration. 1993;164(1):29–43.

6. Hambric S. Power flow and mechanical intensity calculations in structural finite element analysis. Journal of Vibration and Acoustics. 1990;112(4):542–549.

7. Rajamani A, Prabhakaran R. Dynamic response of composite plates with cut-outs, part I: Simply-supported plates. Journal of Sound and Vibration. 1977;54(4):549–564.

8. Lee H, Lim S, Chow S. Free vibration of composite rectangular plates with rectangular cutouts. Composite Structures. 1987;8(1):63–81.

9. Liu Z, Lee H, Lu C. Structural intensity study of plates under low-velocity impact. International Journal of Impact Engineering. 2005;31(8):957–975.

10. Liu Z, Lee H, Lu C. Structural intensity characterization of laminated composite plates subjected to dynamic concentrative force. Chinese Quarterly of Mechanics. 2007;28(2):217–222.

11. Wang D, He P, Liu Z. Structural intensity characterization of composite laminates subjected to impact load. Journal of Shanghai Jiaotong University (Science). 2008;13:375–380.

12. Kidawa-Kukla J. Vibration of a beam induced by harmonic motion of a heat source. Journal of Sound and Vibration. 1997;205(2):213–222.

13. Vance JM, Gibson R, Krishna-Murty A, Boreai A, Huebner K. Dynamic stiffness and damping of fiber-reinforced composite materials. The Shock and Vibration Digest. Volume 9, Number 2. February 1977. Document; 1977.

14. Adams R, Bacon D. Effect of fibre orientation and laminate geometry on the dynamic properties of CFRP. Journal of Composite Materials. 1973;7(4):402–428.

15. Ni R, Adams R. The damping and dynamic moduli of symmetric laminated composite beamsâĂŤtheoretical and experimental results. Journal of Composite Materials. 1984;18(2):104–121.

16. Adams R, Maheri M. Dynamic flexural properties of anisotropic fibrous composite beams. Composites Science and Technology. 1994;50(4):497–514.

17. Lin D, Ni R, Adams R. Prediction and measurement of the vibrational damping parameters of carbon and glass fibre-reinforced plastics plates. Journal of Composite Materials. 1984;18(2):132–152.

18. Maheri M, Adams R. Finite-element prediction of modal response of damped layered composite panels. Composites Science and Technology. 1995;55(1):13–23.

19. Yim J. A damping analysis of composite laminates using the closed form expression for the basic damping of Poisson's ratio. Composite Structures. 1999;46(4):405–411.

20. Yim JH, Jang BZ. An analytical method for prediction of the damping in symmetric balanced laminated composites. Polymer Composites. 1999;20(2):192–199.

21. Yim J, Gillespie Jr J. Damping characteristics of 0 and 90 AS4/3501-6 unidirectional laminates including the transverse shear effect. Composite Structures. 2000;50(3):217–225.

22. Maheri M, Adams R, Hugon J. Vibration damping in sandwich panels. Journal of Materials Science. 2008;43(20):6604–6618.

23. Berthelot J. Dynamics of composite materials and structures. Institute for Advanced Materials and Mechanics, Springer, New York. 1999;.

24. Yang J, Xiong J, Ma L, Wang B, Zhang G, Wu L. Vibration and damping characteristics of hybrid carbon fiber composite pyramidal truss sandwich panels with viscoelastic layers. Composite Structures. 2013;106:570–580.

25. Bert CW. Composite Materials: A Survey of the Damping Capacity of Fiber-Reinforced Composites. Document; 1980.

26. Zabaras N, Pervez T. Viscous damping approximation of laminated anisotropic composite plates using the finite element method. Computer Methods in Applied Mechanics and Engineering. 1990;81(3):291–316.
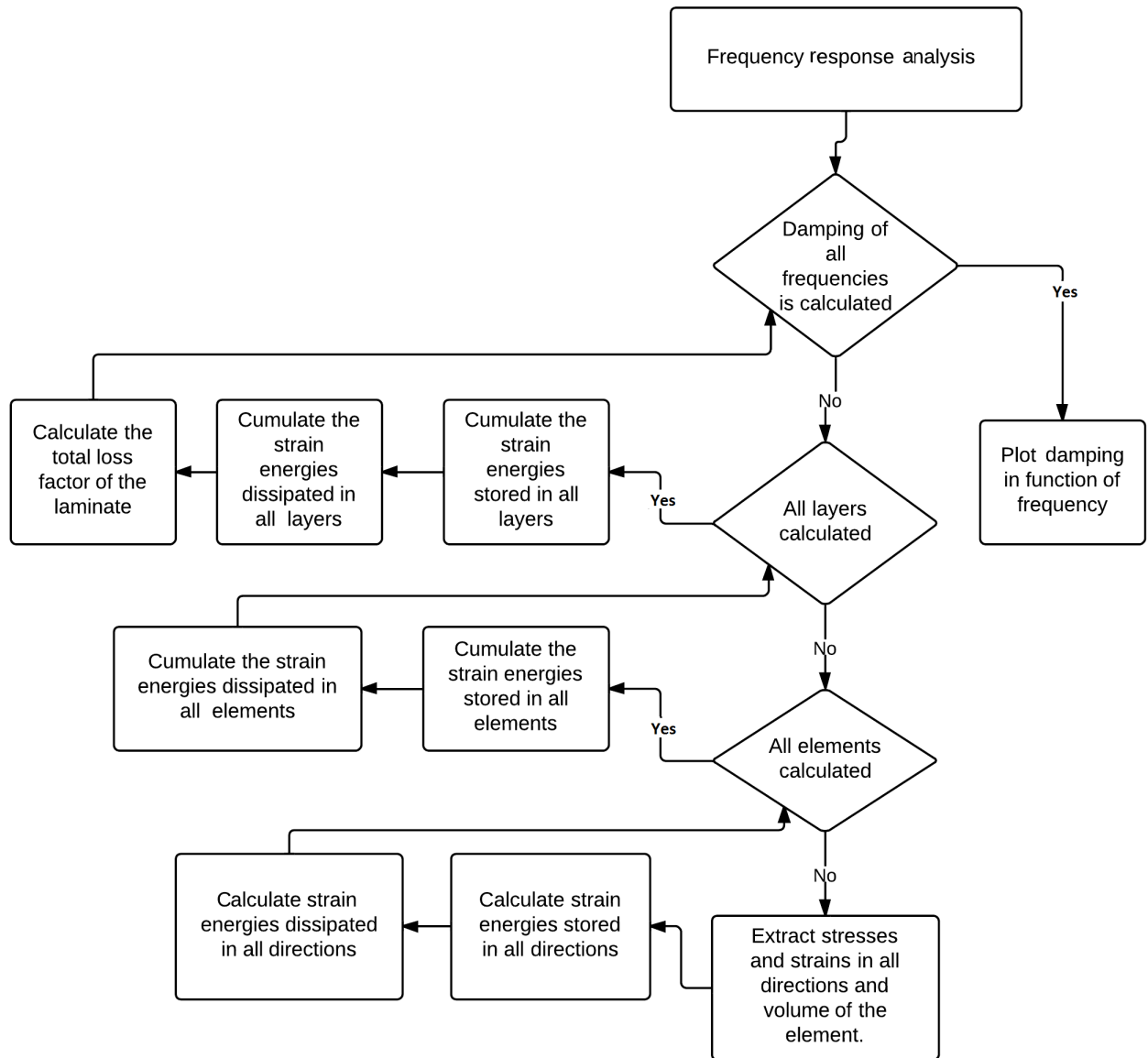
Figure 1 – Procedure to calculate the damping by the modal strain energy method.
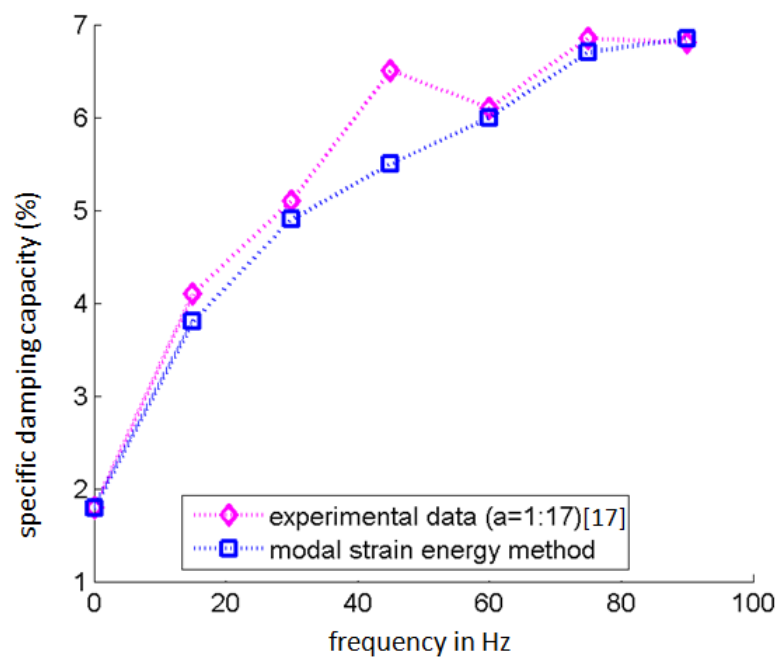
Figure 2 – Variation of specific damping capacity with fiber orientation for a glass/epoxy(fiberdux 913 G) laminate with a unidirectional layup of $[\theta^{\circ}]_8$.

W/m²

>0.0004
0.00036
0.00032
0.00028
0.00024
0.0002
0.00016
0.00012
8e-005
4e-005
<0

a) composite D: variable damping

b) composite D: constant damping
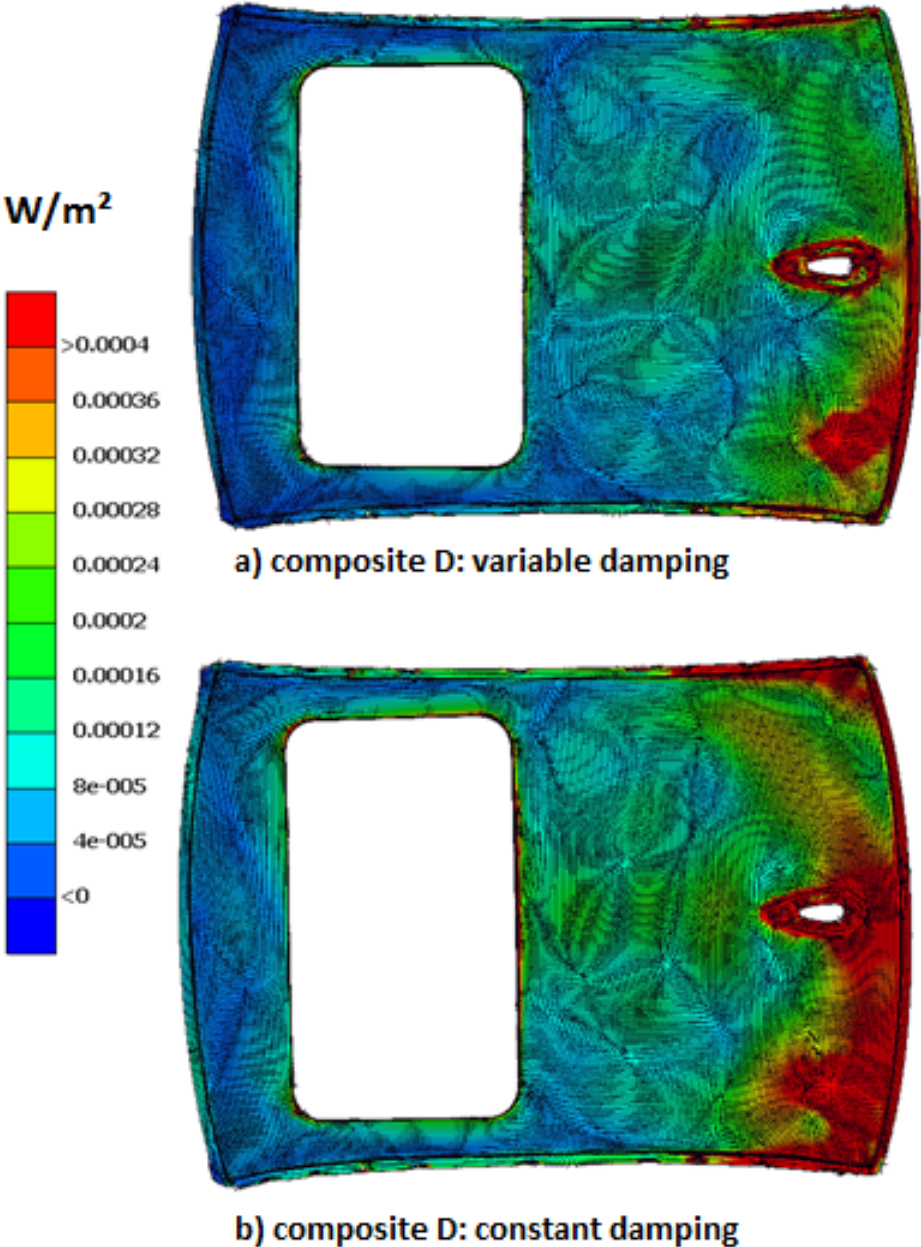
Figure 3 – Effect of the damping on averaged structural intensity from 0 to 600 Hz.
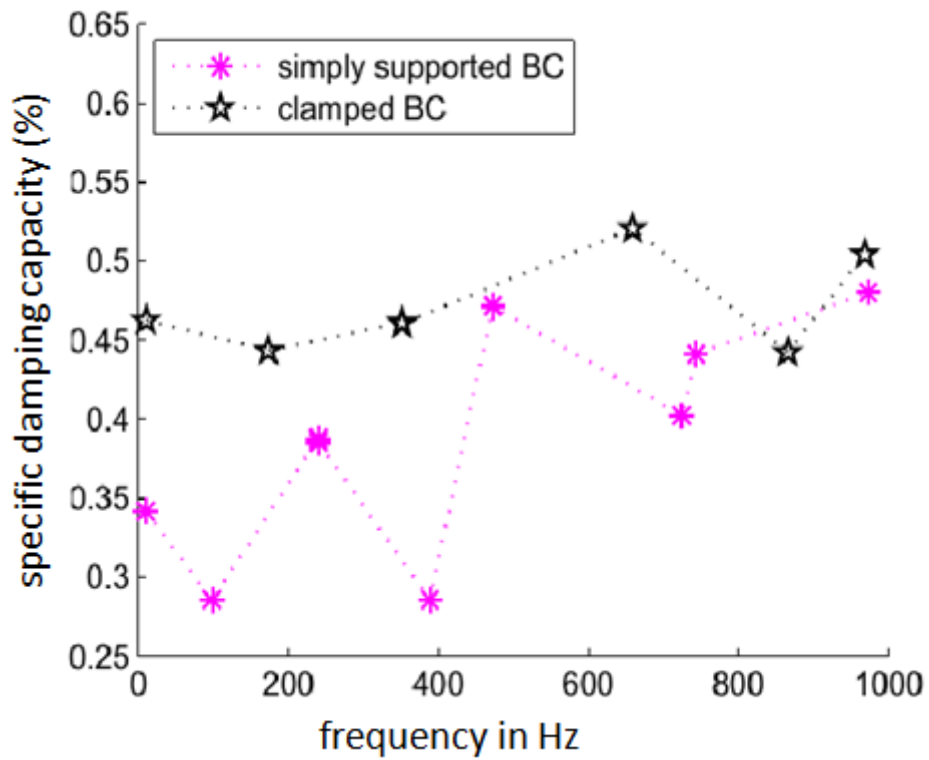
Figure 4 – Effect of boundary conditions on the damping.
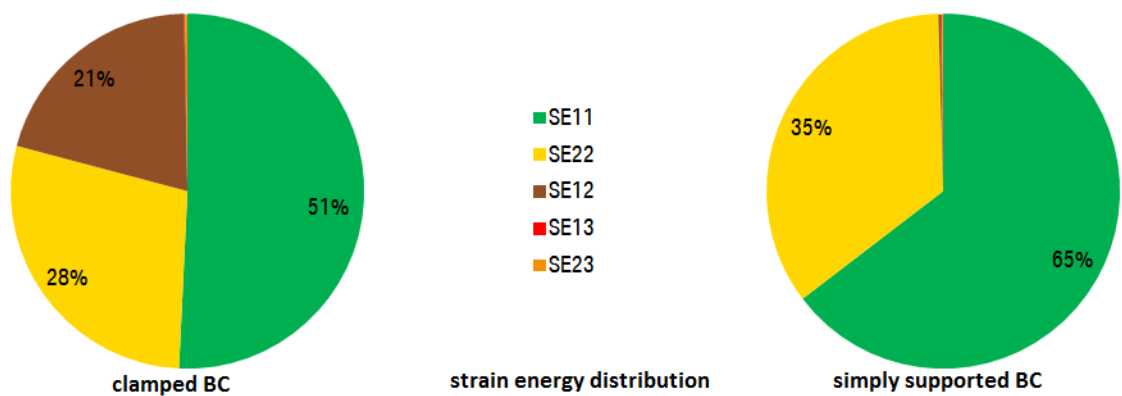
Figure 5 – Distribution of the strain energy as a function of the boundary conditions.
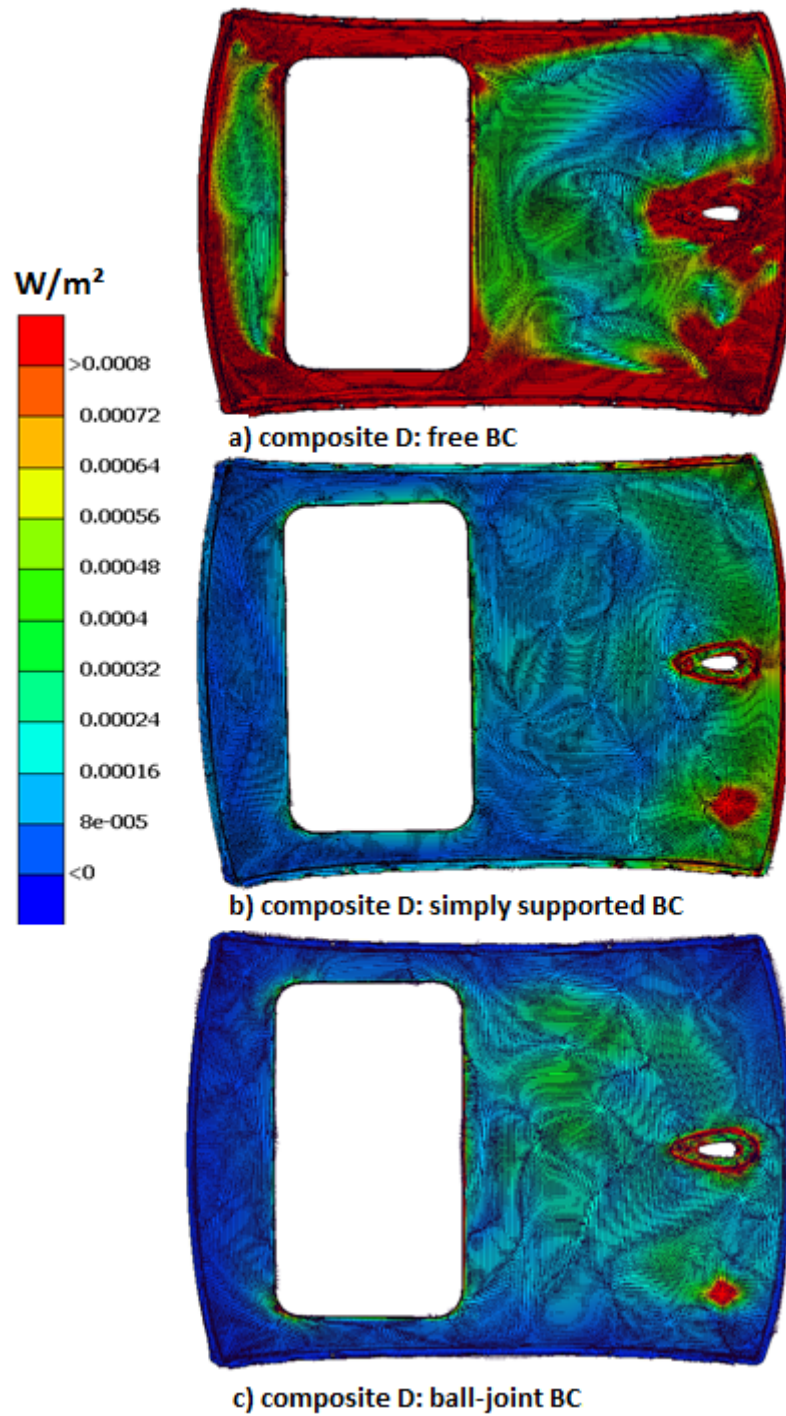
Figure 6 – Effect of boundary conditions on the vibrational energy flow.
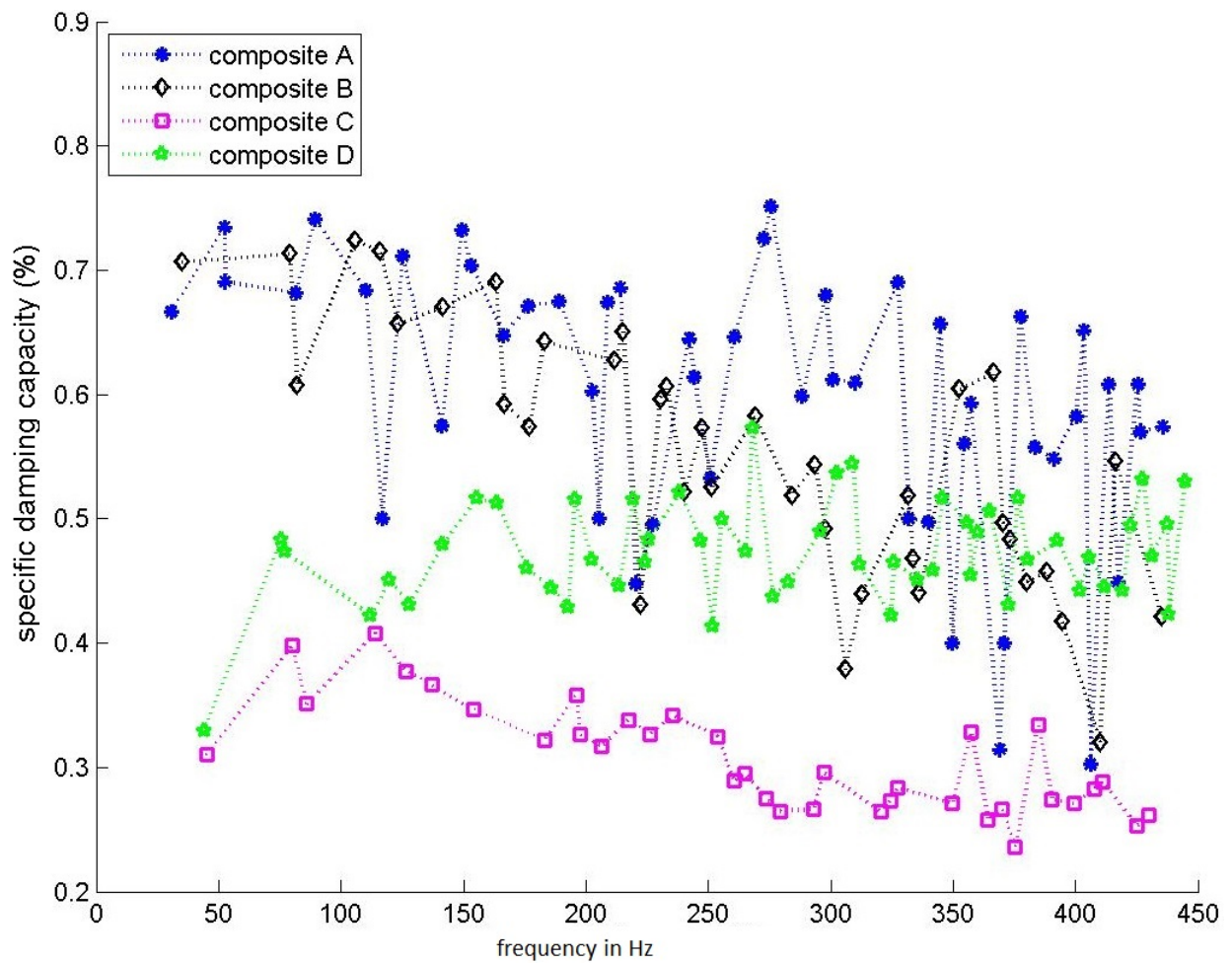
Figure 7 – Effect of composite lay-ups on the damping.
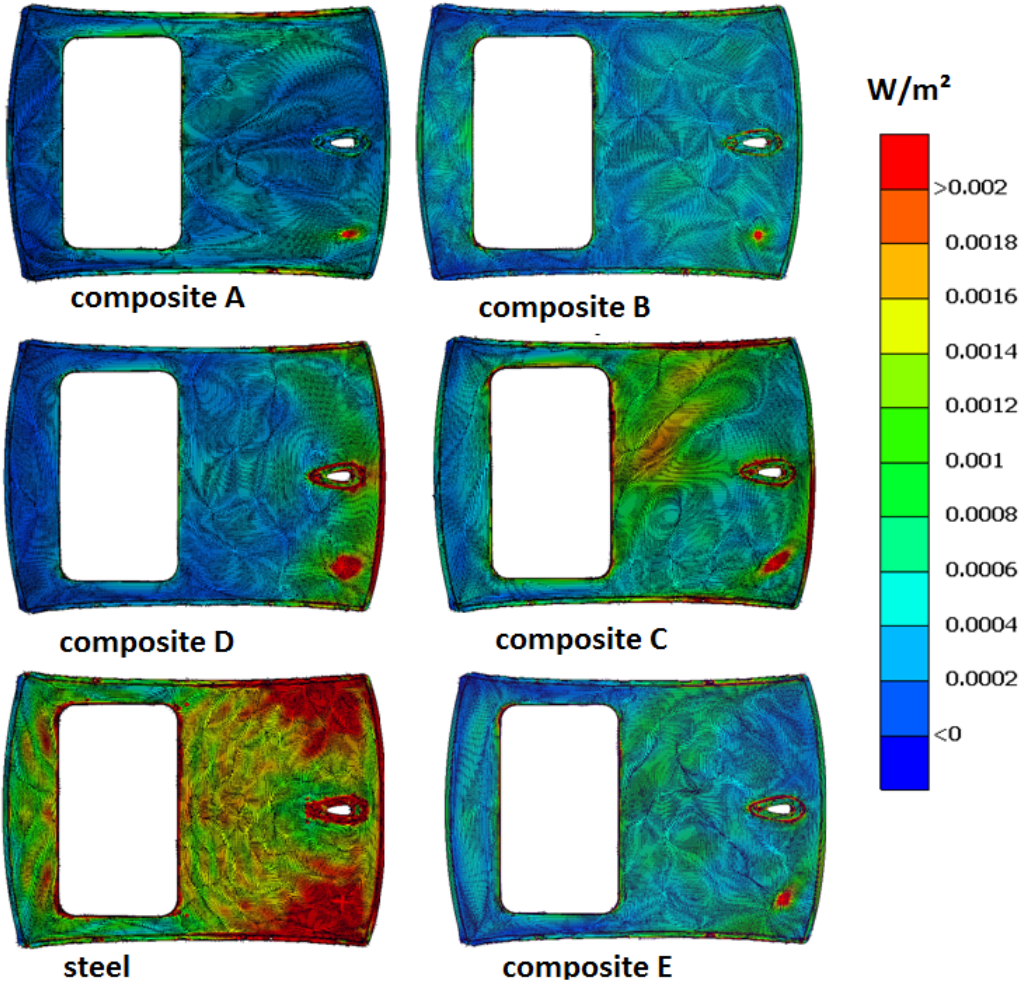
Figure 8 – Effect of the Composite Lay-up on the Damping.